ELSEVIER

Longitudinal heat conduction effects on a vertical thin plate in a steady laminar condensation process

F. Méndez
Facultad de Ingeniería, UNAM, Mexico DF, Mexico

C. Treviño
Facultad de Ciencias, UNAM, Mexico DF, Mexico

In this paper, we analyze the steady-state condensation process of a saturated vapor in contact with one side of a vertical thin plate, caused by an uniform cooling rate on the other surface of the plate. The effects of both longitudinal and transverse heat conduction in the plate are considered. The momentum and energy balance equations are reduced to a system of three differential equations with four parameters: the Prandtl (Pr) and Jakob (Ja) numbers, a nondimensional plate thermal conductivity α, and the aspect ratio of the plate ε. To obtain the evolution of the condensed layer thickness and the related temperature of the plate as a function of the longitudinal coordinate position, the coupled balance equations are integrated in the asymptotic limit $Ja \to 0$, including the cases of very good and poor conducting plates. The results obtained indicate that the effect of the longitudinal heat conduction through the plate on the condensed layer thickness changes from a profile $x^{1/4}$ for a good conducting plate to $x^{1/3}$ for a poor conducting plate.

Keywords: condensation; conjugate heat transfer

Introduction

Since the classical work of Nusselt (1916), the theoretical studies of laminar film condensation have received considerable attention in the literature. In general, development in this area has concentrated on those investigations in which the relative importance of additional complicating factors is revealed. In this sense, the natural convection condensation process on vertical plates is not an exceptional case, and relevant analyses including inertia, convection, and shear stress effects at the condensate surface, show that the simple Nusselt results are surprisingly accurate over a wide range of conditions. A particular contribution on this issue comes from Rohsenow (1956), wherein he modified Nusselt's analysis including the energy convection in the heat balance equation. However, his analysis did not include the inertial forces as was done by Bromley (1952), using other alternative procedure.

In an effort to obtain a better approximation, Sparrow and Gregg (1959), introducing a boundary-layer treatment and similarity transformation of the governing equations, showed numerically that the inertial effects on heat transfer are not important if the Prandtl number is larger or equal to 10 and was quite small for even a Prandtl number of order unity. Later, Chen (1961), solved integral forms of the boundary-layer equations by perturbation methods, including the retarding effect of vapor shear stress on the condensate film. A comparison of the results obtained by Sparrow and Gregg with those obtained by Chen shows that the influence of surface shear stress is negligible at higher Prandtl numbers. To show the influence of this effect more accurately, Koh et al. (1961) incorporated the interfacial shear stress by using the simultaneous solution of the vapor and condensate boundary-layer equations and concluded that the effect of the shear stress is significant only when the condensation rate is sufficiently high. Similar results were obtained by Rose (1988), using a similarity approach confirming the previous problem solved by Chen and gave even more accurate expressions for the Nusselt number. The state-of-the-art of the laminar film condensation on vertical plates and other condensing processes was reported in Merte (1973), and more recently in Rose (1988) and Tanasawa (1991).

The foregoing studies particularly address isothermal vertical plates with known temperature. However, theoretical studies of film condensation processes with nonisothermal conditions had received little attention in the literature. Patankar and Sparrow (1979) solved the problem of condensation on an extended surface by considering the heat conduction in a fin coupled with the condensation process. Their numerical solution of the governing equations confirms the physical influence of a nonisothermal extended surface over the condensing process. Subsequently, it was shown by Wilkins (1980) that an explicit analytical solution is possible for the formulation of Patankar and Sparrow. The main conclusion of the article is that the studies of condensation on extended surfaces form a class by themselves, and an estimation of the surface area requirements of the condenser, using the classical Nusselt analysis for an isothermal case, is inappropriate.

Address reprint requests to Prof. Cesar Treviño, Departamento de Física, Ciudad Universitaria 04510, Mexico DF, Mexico.

Received 7 October 1995; accepted 24 April 1996

Int. J. Heat and Fluid Flow 17: 517–525, 1996

655 Avenue of the Americas, New York, NY 10010

0142-727X/96/$15.00
PII S0142-727X(96)00058-9

To extend these particular cases with nonisothermal conditions, Brouwers (1989) performed an analysis of the condensation of a pure saturated vapor on a cooled channel plate, including the interaction between the cooling liquid, the condensate, and the vapor. His results confirm that this interaction must be taken into account in order to have a more realistic model in this type of processes.

The main objective of this paper is to analyze, using asymptotic as well numerical methods, the laminar film condensation process over a nonisothermal vertical flat plate with finite thickness and thermal conductivity. The wall energy governing equation is coupled with the condensing process at one vertical face of the flat plate, while the flat plate is cooled with a known constant external flux q_e at the other vertical face.

Order-of-magnitude estimates

The physical model under study is shown in Figure 1. A thin vertical plate of length L and thickness h is placed to the right in a stagnant atmosphere filled with saturated vapor with a temperature T_s. Its upper right corner coincides with the origin of a Cartesian coordinate system whose y-axis points in the direction normal to the plate, and its x-axis points down in the plate's longitudinal direction; that is, in the direction of gravity. A known heat flux per unit length, q_e is taken away from the other side of the plate. For simplicity, we assume throughout the paper that both edges of the plate are adiabatic. A thin condensed laminar layer develops with increasing thickness downstream falling by gravity. The density of the condensed fluid, ρ_l is assumed to be constant and much larger than the vapor density. An order-of-magnitude analysis shows that the condensed fluid longitudinal velocity is of the order $u_c \sim (g/\nu_l)\delta^2(x) \sim \sqrt{gL\mathrm{Ja}}$, where δ is the condensed layer thickness, g is the gravity acceleration, ν_l corresponds to the kinematic coefficient of viscosity ($=\mu_l/\rho_l$), and Ja corresponds to the appropriate Jakob number, representing the ratio of the sensible heat energy absorbed by the liquid to the latent heat of the liquid during condensation, defined by

$$\mathrm{Ja} = \left(\frac{3q_e L^{\frac{1}{4}}}{\rho_l h_{fg} g^{\frac{1}{4}} \nu^{\frac{1}{2}}} \right)^{4/3} \tag{1}$$

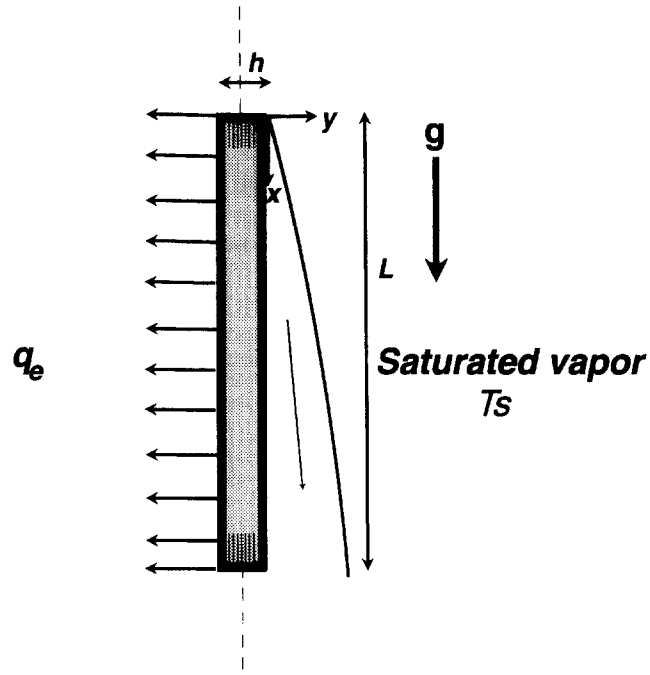

Figure 1 Schematic diagram of the studied physical model

Here h_{fg} corresponds to the latent heat of condensation. This definition of the Jakob number is derived from the classical form, using the known heat flux instead of the temperature variation in the condensed film. The condensed mass flow rate is then of the order of $\dot{m} \sim (\rho_l g/\nu_l)\delta^3(x)$. The production rate of condensed fluid can be obtained from the thermal energy relationship at the condensed vapor interface as $d\dot{m}/dx \sim q_e/h_{fg}$. From all these relationships, we observe that the thickness of the condensed layer related to the length of the plate is

$$\frac{\delta}{L} \sim \left(\frac{\mathrm{Ja}}{\gamma} \right)^{1/4} \quad \text{with} \quad \gamma = \frac{gL^3}{\nu_l^2} \tag{2}$$

Notation

c_l	specific heat of the condensed phase
g	gravity acceleration
h	thickness of the plate
Ja	Jacob number defined in Equation 1
L	length of the plate
m	mass flow rate of condensed fluid
Nu	Nusselt number defined in Equation 7
Pr	Prandtl number
q_e	prescribed heat flux
s	nondimensional stream function defined in Equation 9
s_i	value of g evaluated at $\sigma = 1$
T	temperature
T_s	temperature of the saturated vapor
T_r	characteristic temperature, $T_r = \alpha q_e h/(\varepsilon^2 \lambda_w)$
u, v	nondimensional longitudinal and transversal velocities
u_c	characteristic longitudinal velocity of the condensed fluid
xy	Cartesian coordinates
z	nondimensional transversal coordinate in the plate

Greek

α	heat conduction parameter defined in Equation 5
γ	nondimensional parameter defined in Equation 2
Δ	nondimensional thickness of the condensed layer
δ	thickness of the condensed layer
ζ	nondimensional inner coordinate defined in Equation 49
λ_l	thermal conductivity of the condensed phase
λ_w	plate thermal conductivity
μ_l	dynamic viscosity
ν_l	kinematic coefficient of viscosity
ξ	nondimensional inner coordinate defined in Equation 57
ρ_l	fluid density
σ	nondimensional normalized transversal coordinate
ϕ	nondimensional function introduced in Equation 31
φ	nondimensional inner variable defined in Equation 57
χ	nondimensional longitudinal coordinate defined in Equation 8
ψ	nondimensional inner variable defined in Equation 49

where γ is an unnamed nondimensional parameter (Incropera and DeWitt 1990). Because of the adiabatic edges of the plate, the global heat convected from the saturated vapor to the plate must be the same as the heat diffused from one lateral surface to the other in the plate, that is

$$q_e \sim \frac{\lambda_w \Delta T_w}{h} \sim \frac{\lambda_l \Delta T_l}{\delta} \tag{3}$$

where λ_l and λ_w are the thermal conductivity of the condensed fluid and the plate, respectively. ΔT_w and ΔT_l are the characteristic temperature changes in the transveral direction, for the plate and the condensed fluid, respectively. The total temperature change is then $\Delta T \sim \Delta T_l + \Delta T_w$. Using Eqautions 3, together with 2, we obtain the relative temperature drop on the plate

$$\frac{\Delta T_w}{\Delta T} \sim \frac{1}{1 + \frac{\alpha}{\varepsilon^2}} \tag{4}$$

where α is the heat conduction parameter defined by

$$\alpha = \frac{\lambda_w}{\lambda_l} \frac{h}{L} \left(\frac{\mathrm{Ja}}{\gamma} \right)^{\frac{1}{4}} \tag{5}$$

and ε is the aspect of the plate $\varepsilon = h/L \ll 1$. Parameter α corresponds to the ratio of heat conducted longitudinally by the plate to the heat convected from the saturated vapor. For $\alpha/\varepsilon^2 \gg 1$, the transversal temperature variations in the plate compared with the overall temperature drop ΔT are very small, of order ε^2/α at most. This represents the thermally thin wall limit. On the other hand, for values of α/ε^2 of order unity, the transversal temperature drop in the solid is of the order of magnitude than the overall temperature drop. This represents the thermally thick wall limit. The global temperature change is then of the order

$$\Delta T \sim \frac{q_e h}{\lambda_w} \left(1 + \frac{\alpha}{\varepsilon^2} \right) \tag{6}$$

From Equation 3 we can define a Nusselt number of order unity as

$$\mathrm{Nu} = \frac{q_e h}{\lambda_w \Delta T_w} \sim 1 \tag{7}$$

In this paper, we study the case of $\mathrm{Ja} \ll 1$, which is a good approximation for most of practical cases in condensation (Incropera and DeWitt 1990). Typical values of γ is $\gamma \sim 10^{10}$. The condensed layer thickness is typically $\delta \sim 10^{-3}\ L$, thus the boundary layer approximation is fully justified. The ratio of the thermal conductivities λ_w/λ_l can reach values of 10^3. Therefore, a typical value of α is $\alpha \sim h/L$ and $\alpha/\varepsilon^2 \sim L/h$. In the following section, we deduce the governing equations. The thermally thin approximation is then applied, and the asymptotic limits $\alpha \gg 1$ and $\alpha \ll 1$ are studied. The asymptotic limit $\alpha \gg 1$ is important for this problem, because we can obtain a closed-form solution for the condensed layer thickness evolution, which gives accurate results for values of α of order unity. In Appendix B we analyze the case of a thermally thick wall.

Formulation

We introduce the following nondimensional variables

$$\theta_w = \frac{T_s - T_w}{T_r}, \theta = \frac{T_s - T}{T_r}, \chi = \frac{x}{L}, z = \frac{y}{h}, \sigma = \frac{y}{\delta} \tag{8}$$

$$\Delta = \frac{\delta}{L} \left(\frac{\gamma}{\mathrm{Ja}} \right)^{1/4}, u = \frac{\bar{u}}{\sqrt{gL\mathrm{Ja}}} = \Delta^3 \frac{\partial s}{\partial \eta}; v = \frac{\gamma^{\frac{1}{4}} \bar{v}}{\mathrm{Ja}^{\frac{3}{4}} \sqrt{gL}} = -\frac{\partial (\Delta^3 s)}{\partial \chi} \tag{9}$$

where T_r represents the characteristic global temperature change dictated by Equation 6 and is given by

$$T_r = \frac{\alpha}{\varepsilon^2} \frac{q_e h}{\lambda_w}$$

$\bar{u}$ and $\bar{v}$ represent the longitudinal and transversal velocity components in physical units, s is the nondimensional stream function, and $\Delta(\chi)$ represents the unknown nondimensional thickness of the condensed layer to be obtained as part of the solution of the problem. The energy equation for the plate is given by the nondimensional Laplace equation

$$\frac{\partial^2 \theta_w}{\partial \chi^2} + \frac{1}{\varepsilon^2} \frac{\partial^2 \theta_w}{\partial z^2} = 0 \tag{10}$$

The adiabatic boundary conditions at both edges are

$$\frac{\partial \theta_w}{\partial \chi} = 0, \quad \text{for} \quad \chi = 0 \quad \text{and} \quad 1 \tag{11}$$

The other two boundary conditions are obtained from equating the heat fluxes at both faces of the plate and assuming continuity for the temperature at the solid–condensed fluid interface

$$\left. \frac{\partial \theta_w}{\partial z} \right|_{z=0} = \frac{\varepsilon^2}{\alpha \Delta} \left. \frac{\partial \theta}{\partial \sigma} \right|_{\sigma=0}, \left. \frac{\partial \theta_w}{\partial z} \right|_{z=-1} = -\frac{\varepsilon^2}{\alpha} \tag{12}$$

and

$$\theta_w(\chi, z=0) = \theta(\chi, \sigma=0) \tag{13}$$

For the condensed phase, the nondimensional governing equations are

$$\frac{\partial^3 s}{\partial \sigma^3} + 1 = \mathrm{Ja}\Delta^4 \left\{ \frac{\partial s}{\partial \sigma} \frac{\partial^2 s}{\partial \chi \partial \sigma} - \frac{\partial s}{\partial \chi} \frac{\partial^2 s}{\partial \sigma^2} + \frac{3}{\Delta} \frac{d\Delta}{d\chi} \left[\left(\frac{\partial s}{\partial \sigma} \right)^2 - s \frac{\partial^2 s}{\partial \sigma^2} \right] \right\} \tag{14}$$

$$\frac{\partial^2 \theta}{\partial \sigma^2} = \mathrm{JaPr}\Delta^4 \left\{ \frac{\partial s}{\partial \sigma} \frac{\partial \theta}{\partial \chi} - \frac{\partial s}{\partial \chi} \frac{\partial \theta}{\partial \sigma} - \frac{3}{\Delta} \frac{d\Delta}{d\chi} s \frac{\partial \theta}{\partial \sigma} \right\} \tag{15}$$

where Pr corresponds to the Prandtl number given by $\mathrm{Pr} = \mu_l c_l / \lambda_l$. The corresponding boundary conditions now take the form

$$\theta(\chi, \sigma = 0) = \theta_w(\chi, 0); s(\chi, \sigma = 0) = 0; \left.\frac{\partial s}{\partial \sigma}\right|_{\sigma = 0} = 0 \tag{16}$$

$$\theta(\chi, \sigma = 1) = 0; \left.\frac{\partial^2 s}{\partial \sigma^2}\right|_{\sigma = 1} = 0 \tag{17}$$

together with $\Delta(\chi = 0) = 0$. The energy balance at the condensed vapor interface is provided by the following relationship

$$3\Delta \frac{\mathrm{d}(\Delta^3 s_i(\chi))}{\mathrm{d}\chi} = -\left.\frac{\partial \theta}{\partial \sigma}\right|_{\sigma = 1} \tag{18}$$

where s_i is the value of s evaluated at the condensed-vapor interface, $\sigma = 1$. The second condition of Equation 17 arises from the balance of tangential shear stress at the interface (Koh et al. 1961).

The system of Equations 14 to 18, together with the Laplace Equation 10 and the corresponding boundary conditions contains four differential equations with four unknowns, $s(\chi, \sigma)$, $\theta(\chi, \sigma)$, $\Delta(\chi)$, and $\theta_w(\chi, z)$ with four different nondimensional parameters, Ja, Pr α, and ε. In the following sections, we analyze the realistic case $\mathrm{Ja} \to 0$, with Prandtl number such as $\mathrm{Pr} \ll \mathrm{Ja}^{-1}$. For small values of Ja, the convective terms for the condensed fluid momentum 14 can be neglected, giving

$$s(\sigma) = \frac{1}{2}\sigma^2\left(1 - \frac{\sigma}{3}\right) \text{ or } s_i = \frac{1}{3} \tag{19}$$

Thermally thin wall regime ($\alpha/\varepsilon^2 \gg 1$)

For the important case of a thermally thin wall ($\alpha/\varepsilon^2 \gg 1$), the temperature variations in the transversal direction of the plate can be neglected as shown in the order of magnitude section. The energy balance Equation 10 can be integrated in the transversal direction and after applying the boundary conditions at both lateral surfaces, we obtain

$$\alpha \frac{\mathrm{d}^2 \theta_w}{\mathrm{d}\chi^2} + \frac{1}{\Delta}\left.\frac{\partial \theta}{\partial \sigma}\right|_{\sigma = 0} = -1 \tag{20}$$

to be solved with the adiabatic conditions at both edges.

Prandtl number $\ll \mathrm{Ja}^{-1}$

In this limit, the governing Equations 15, 18, and 20 can be solved using the following perturbation expansions

$$\theta = \theta_0(\chi, \sigma) + \mathrm{JaPr}\,\theta_1(\chi, \sigma) + O(\mathrm{Ja}) + O(\mathrm{JaPr})^2 \tag{21}$$

$$\Delta = \Delta_0(\chi) + \mathrm{JaPr}\,\Delta_1(\chi) + O(\mathrm{Ja}) + O(\mathrm{JaPr})^2 \tag{22}$$

$$\theta_w = \theta_{w0}(\chi) + \mathrm{JaPr}\,\theta_{w1}(\chi) + O(\mathrm{Ja}) + O(\mathrm{JaPr})^2 \tag{23}$$

Up to terms of order JaPr, the resulting equations for the nondimensional condensed layer thickness take the form

$$\frac{3}{4}\frac{\mathrm{d}(\Delta_0^4)}{\mathrm{d}\chi} = -\left.\frac{\partial \theta_0}{\partial \sigma}\right|_{\sigma = 1} \tag{24}$$

$$3\frac{\mathrm{d}(\Delta_0^3 \Delta_1)}{\mathrm{d}\chi} = -\left.\frac{\partial \theta_1}{\partial \sigma}\right|_{\sigma = 1} \tag{25}$$

where the solution for θ_0 and θ_1 have to be to be found from the equations

$$\frac{\partial^2 \theta_0}{\partial \sigma^2} = 0 \tag{26}$$

$$\frac{\partial^2 \theta_1}{\partial \sigma^2} = \Delta_0^4 \left\{ \frac{\partial s}{\partial \sigma}\frac{\partial \theta_0}{\partial \chi} - \frac{3}{\Delta_0}\frac{\mathrm{d}\Delta_0}{\mathrm{d}\chi} s \frac{\partial \theta_0}{\partial \sigma} \right\} \tag{27}$$

with the boundary and initial conditions

$$\theta_0(\chi, 0) = \theta_{w0}(\chi) \text{ and } \Delta_0(0) = 0$$

$$\theta_1(\chi, 0) = \theta_{w1}(\chi) \text{ and } \Delta_1(0) = 0$$

The solution for θ_0 is represented by a linear profile

$$\theta_0(\chi, \sigma) = \theta_{w0}(1 - \sigma) \tag{28}$$

The corresponding energy equations for the plate are up to the first order

$$\alpha \frac{\mathrm{d}^2 \theta_{w0}}{\mathrm{d}\chi^2} - \frac{\theta_{w0}}{\Delta_0} = -1 \tag{29}$$

$$\alpha \frac{\mathrm{d}^2 \theta_{w1}}{\mathrm{d}\chi^2} - \frac{\Delta_1}{\Delta_0^2}\left.\frac{\partial \theta_0}{\partial \sigma}\right|_{\sigma = 0} + \frac{1}{\Delta_0}\left.\frac{\partial \theta_1}{\partial \sigma}\right|_{\sigma = 0} = 0 \tag{30}$$

to be solved with adiabatic boundary conditions $\mathrm{d}\theta_{wn}/\mathrm{d}\chi)_{\chi = 0, 1} = 0$. The leading order system of Equations 24 and 29 can be reduced to a single differential equation, which gives the evolution of the condensed layer thickness as a function of the longitudinal coordinate

$$\alpha \frac{\mathrm{d}^3 \phi}{\mathrm{d}\chi^3} - \frac{1}{\phi^{\frac{1}{4}}}\frac{\mathrm{d}\phi}{\mathrm{d}\chi} = -\frac{4}{3} \tag{31}$$

where $\phi = \Delta_0^4$ and $\theta_{w0} = (3/4)\mathrm{d}\phi/\mathrm{d}\chi$. This nonlinear equation contains only the parameter α. This equation must be solved numerically (see Appendix A) or using perturbation techniques for large and small values of the parameter α, as shown below.

Solution for $\alpha \to \infty$. This is a regular limit. For very large values of the parameter α, the leading term nondimensional temperature of the plate $\mathrm{d}\phi/\mathrm{d}\chi$ changes very little (of order of α^{-1}) in the longitudinal direction, as shown in the order of magnitude section. Assuming a solution of the form

$$\phi(\chi) = \phi_0(\chi) + \sum_{j=1}^{\infty} \alpha^{-j} \phi_j(\chi) \tag{32}$$

and introducing this relationship into Equation 31, we obtain after collecting terms of the same power of α^{-j}, the following sets of equations

$$\frac{d^3\phi_0}{d\chi^3} = 0 \tag{33}$$

$$\frac{d^3\phi_1}{d\chi^3} = \frac{1}{\phi_0^{\frac{1}{4}}}\frac{d\phi_0}{\partial\chi} - \frac{4}{3} \tag{34}$$

$$\frac{d^3\phi_2}{d\chi^3} = \frac{1}{\phi_0^{\frac{1}{4}}}\frac{d\phi_1}{\partial\chi} - \frac{1}{4}\frac{\phi_1}{\phi_0^{\frac{5}{4}}}\frac{d\phi_0}{\partial\chi} \tag{35}$$

etc., with the following initial and boundary conditions

$$\phi_i(0) = 0; \left.\frac{d^2\phi_i}{d\chi^2}\right|_{\chi=0,1} = 0, \qquad \text{for all} \quad i \tag{36}$$

Solving Equations 33 and 36 gives $\phi_0 = C_0\chi$. Integrating Equation 34 in the form

$$\int_0^1 [\,]d\chi$$

and considering the adiabatic conditions at both edges of the plate, we obtain

$$0 = \frac{4}{3}\left(C_0^{\frac{3}{4}} - 1\right) \tag{37}$$

that is $C_0 = 1$. Introducing the solution for ϕ_0 into Equation 34 and integrating three times, we obtain after applying the appropriate initial and boundary conditions

$$\phi_1 = C_1\chi - \frac{2}{9}\chi^3 + \frac{64}{231}\chi^{\frac{11}{4}} \tag{38}$$

where C_1 is an integration constant related to the temperature of the plate at the leading edge and must be determined by solving the next higher-order equation. Integrating of Equation 36 in the form

$$\int_0^1 [\,]d\chi$$

and considering the adiabatic boundaries at both edges of the plate, we obtain $C_1 = -114/2079$. Up to the first order in α^{-1}, the condensed layer thickness is then given by

$$\Delta_0 = \chi^{\frac{1}{4}}\left(1 + \frac{1}{4\alpha}\left(C_1 + \frac{64}{231}\chi^{\frac{7}{4}} - \frac{2}{9}\chi^2\right)\right) + O(\alpha^{-2}) \tag{39}$$

the nondimensional plate temperature is

$$\theta_{w0} = \frac{3}{4}\left[1 + \frac{1}{\alpha}\left(C_1 + \frac{16}{21}\chi^{\frac{7}{4}} - \frac{2}{3}\chi^2\right)\right] + O(\alpha^{-2}) \tag{40}$$

and the Nusselt number is then

$$\mathrm{Nu}_0 = \frac{3}{4\chi^{\frac{1}{4}}}\left[1 + \frac{1}{\alpha}\left(C_1\chi^{\frac{3}{4}} + \frac{160}{231}\chi^{\frac{7}{4}} - \frac{11}{18}\chi^2\right)\right] + O(\alpha^{-2}) \tag{41}$$

The first terms on the right-hand side of the above equations represent the classical Nusselt solution (Nusselt 1916) for an isothermal plate. Therefore, for very large values of the parameter α, the leading order solution is

$$\theta_0 = \frac{3}{4}(1+\sigma), \Delta_0 = \chi^{\frac{1}{4}}, \theta_{w0} = \frac{3}{4} \tag{42}$$

Substituting these relationships into the energy equation for the condensed phase (27), it transforms to

$$\frac{\partial^2\theta_1}{\partial\sigma^2} = \frac{9}{32}\left(\sigma^2 - \frac{\sigma^3}{3}\right) \tag{43}$$

The solution to this equation together with the boundary conditions is readily obtained as

$$\theta_1 = \theta_{w1}(1-\sigma) + \frac{3}{128}(\sigma^4 - \sigma) - \frac{3}{640}(\sigma^5 - \sigma) \tag{44}$$

Similarly, the solution for the first-order correction of the nondimensional plate temperature and thickness of the condensed layer are

$$\theta_{w1} = \frac{51}{3200}; \Delta_1 = -\frac{444}{9600}\chi^{\frac{1}{4}} \tag{45}$$

Finally, the global solution up to terms of order α^{-1} or JaPr, is then given by

$$\Delta = \chi^{\frac{1}{4}}\left(1 + \frac{1}{4\alpha}\left(-\frac{114}{2079} + \frac{64}{231}\chi^{\frac{7}{4}} - \frac{2}{9}\chi^2\right) - \frac{444}{9600}\mathrm{JaPr}\right) + O(\alpha^{-2}, \mathrm{Ja}, \mathrm{Ja}^2\mathrm{Pr}^2) \tag{46}$$

$$\theta_w = \frac{3}{4}\left(1 + \frac{1}{\alpha}\left(-\frac{114}{2079} + \frac{16}{21}\chi^{\frac{7}{4}} - \frac{2}{3}\chi^2\right) - \frac{204}{9600}\mathrm{JaPr}\right) + O(\alpha^{-2}, \mathrm{Ja}, \mathrm{Ja}^2\mathrm{Pr}^2) \tag{47}$$

$$\mathrm{Nu} = \frac{3}{4\chi^{\frac{1}{4}}}\left(1 + \frac{1}{\alpha}\left(-\frac{114}{2079}\chi^{\frac{3}{4}} + \frac{160}{231}\chi^{\frac{7}{4}} - \frac{11}{18}\chi^2\right) + \frac{888}{9600}\mathrm{JaPr}\right) + O(\alpha^{-2}, \mathrm{Ja}, \mathrm{Ja}^2\mathrm{Pr}^2) \tag{48}$$

Solution for $\alpha \to 0$. For small values of α compared with unity, the longitudinal heat conduction can be neglected. However, this is a singular limit due to appearance of two layers close to both edges in order to satisfy the adiabatic conditions. Close to the leading edge there is a boundary layer of thickness of the order of $\chi \sim \alpha^{\frac{3}{5}}$. Outside this inner zone, longitudinal heat conduction through the plate is negligible, obtaining to the leading order $\phi_e \sim \chi^{\frac{4}{3}}$. Introducing the following inner variables

$$\zeta = \left(\frac{3}{4\alpha^3}\right)^{\frac{1}{5}}\chi; \psi = \left(\frac{9}{16\alpha}\right)^{\frac{4}{5}}\phi \tag{49}$$

the evolution Equation 31 for the condensed layer thickness transform to the parameter-free equation

$$\frac{d^3\psi}{d\zeta^3} - \frac{1}{\psi^{\frac{1}{4}}}\frac{d\psi}{d\zeta} = -1 \tag{50}$$

with the initial conditions given by

$$\psi(0) = \left.\frac{d^2\psi}{d\zeta^2}\right|_{\zeta=0} = 0 \tag{51}$$

Another condition is to be obtained after matching with the outer zone solution,

$$\psi(\zeta \to \infty) \sim \left(\frac{3}{4}\zeta\right)^{\frac{4}{3}} \tag{52}$$

The general behavior of Equations 50 to 52 can be found in Appendix A. There is only one value for the initial slope which satisfy the matching condition for large values of ζ and is given by (see Appendix A) $(d\psi/d\zeta)_0 \simeq 0.7944\ldots$. Close to the leading edge, the leading-order nondimensional thickness of the condensed layer is given by

$$\Delta_0 - (0.7944\ldots)^{\frac{1}{4}}\left(\frac{4}{3}\right)^{\frac{7}{20}}\alpha^{\frac{1}{20}}\chi^{\frac{1}{4}} \tag{53}$$

changing the behavior at the end of the boundary layer as

$$\Delta_0 \simeq \chi^{\frac{1}{3}} \tag{54}$$

The nondimensional temperature at the leading edge of the plate decreases with α as $\alpha^{1/5}$ and is then given by

$$\theta_{w0l} = (0.7944\ldots)\left(\frac{4}{3}\right)^{\frac{2}{5}}\alpha^{\frac{1}{5}}, \text{ for } \alpha \to 0 \tag{55}$$

The Nusselt number changes in this transition layer from

$$\mathrm{Nu}_0 \simeq \frac{(0.7944\ldots)^{\frac{3}{4}}\left(\frac{4}{3}\right)^{\frac{1}{20}}\alpha^{\frac{3}{20}}}{\chi^{\frac{1}{4}}} \tag{56}$$

at the beginning reaching asymptotically $\mathrm{Nu} \simeq 1$ at the end.

On the other hand, close to the trailing edge we have a thin transition layer of order $(1-\chi) \sim \sqrt{\alpha}$, where the temperature gradient goes to zero as $\chi \to 1$. To study this layer, we first introduce the following inner variables

$$\xi = \frac{1-\chi}{\sqrt{\alpha}}; \varphi = \frac{3 - \frac{9}{4}\frac{d\phi}{d\chi}}{\sqrt{\alpha}} \tag{57}$$

and obtain the following transformed linear equation

$$\frac{d^2\varphi}{d\xi^2} - \varphi = -\xi \tag{58}$$

with the conditions

$$\left.\frac{d\varphi}{d\xi}\right|_{\xi=0} = 0 \text{ and } \varphi(\xi \to \infty) \sim \xi \tag{59}$$

The first condition arises from the adiabaticity at the trailing edge of the plate, while the second one comes from matching with the outer solution ($\alpha = 0$). The solution of Equations (58) and (59) is readily obtained and is given by

$$\varphi = \xi + \exp(-\xi) \tag{60}$$

The nondimensional temperature of the plate close to the trailing edge for small values of α in terms of the outer variables is then given by

$$\theta_{w0} = \chi^{\frac{1}{3}} - \frac{4\sqrt{\alpha}}{9}\exp\left(-\frac{1-\chi}{\sqrt{\alpha}}\right) \tag{61}$$

while the local Nusselt number can be written as

$$\mathrm{Nu}_0 = 1 - \frac{4\sqrt{\alpha}}{9\chi^{\frac{1}{3}}}\exp\left(-\frac{1-\chi}{\sqrt{\alpha}}\right) \tag{62}$$

Therefore, the leading term outer solution are given by

$$\theta_0 = \chi^{\frac{1}{3}}(1-\sigma), \Delta_0 = \chi^{\frac{1}{3}} \text{ and } \theta_{w0} = \chi^{\frac{1}{3}} \tag{63}$$

Substituting these relationships into the energy equation for the condensed phase 27, it transforms to

$$\frac{\partial^2\theta_1}{\partial\sigma^2} = \chi^{\frac{2}{3}}\left(-\frac{\sigma}{3} + \sigma^2 - \frac{\sigma^3}{3}\right) \tag{64}$$

The solution to this equation together with the boundary conditions is

$$\theta_1 = \theta_{w1}(1-\sigma) + \chi^{\frac{2}{3}}\left[\frac{1}{18}(\sigma - \sigma^3) + \frac{1}{12}(\sigma^4 - \sigma) - \frac{1}{60}(\sigma^5 - \sigma)\right] \tag{65}$$

Similarly, the solution for the first-order correction of the nondimensional plate temperature and thickness of the condensed layer are

$$\theta_{w1} = \frac{1}{540}\chi^{\frac{5}{3}}; \Delta_1 = -\frac{1}{540}\chi^{\frac{5}{3}} - \frac{12}{1080}\chi^{\frac{2}{3}} \tag{66}$$

The global solution for the case of $\alpha \to 0$ is then given by (neglecting the influences of both layers close to the edges of the plate)

$$\Delta = \chi^{\frac{1}{3}}\left(1 - \left(\frac{1}{540}\chi^{\frac{4}{3}} + \frac{1}{90}\chi^{\frac{1}{3}}\right)\mathrm{JaPr}\right) + O(\mathrm{Ja}, \mathrm{Ja}^2\mathrm{Pr}^2) \tag{67}$$

$$\theta_w = \chi^{\frac{1}{3}}\left(1 + \frac{1}{540}\chi^{\frac{4}{3}}\mathrm{JaPr}\right) + O(\mathrm{Ja}, \mathrm{Ja}^2\mathrm{Pr}^2) \tag{68}$$

$$\mathrm{Nu} = 1 + \frac{1}{90}\chi^{\frac{2}{3}}\left(1 + \frac{1}{6}\chi\right)\mathrm{JaPr} + O(\mathrm{Ja}, \mathrm{Ja}^2\mathrm{Pr}^2) \tag{69}$$

Results and conclusions

For values of α of order unity, it is necessary to solve numerically the governing Equation (31), with the respective boundary and initial conditions, for the thermally thin wall regime. The numerical scheme used here is described in Appendix A. Figure 2 shows the evolution of nondimensional temperature at the plate as a function of χ for different values of the parameter α in the limit $Ja \to 0$ and Pr of order unity. There is good agreement between the asymptotic and the numerical solution even for value of α of order unity. As we can see, the nondimensional temperature of the plate decreases in the frontal regions of the plate and increases behind as the value of α decreases. The leading term solution for $\alpha \to \infty$ is the classical Nusselt solution, indicating clearly the influence of the parameter α on the process. Figure 3 shows the nondimensional condensed layer thickness as a function of χ for different values of α for the same limit. At the trailing edge of the plate, the thickness as well the condensed mass flow rate are the same for all values of α, for Prandtl numbers of order unity. This is because we prescribed the heat flux and assumed adiabatic edges of the plate as well as the heat flux in the condensed fluid is invariant in the transversal direction. This is not the case when the Prandtl number is large enough to consider the convective terms in the energy equation for the condensed phase. As the Prandtl number increases, both the thickness of the condensed layer as well as the mass flow rate decreases, as shown in the first-order corrections in Equations 46 and 67, for large and small values of α, respectively. For large values of α, the condensed layer thickness varies like $x^{1/4}$, while for small values, we obtained the behavior like $x^{1/3}$. The same behavior is obtained using both thermally thin and thick wall approximations (see Appendix B). For finite values of α, the behavior changes from $x^{1/4}$ close to the leading edge to $x^{1/3}$ towards the trailing edge. Finally, Figure 4 shows the Nusselt number as a function of χ for different values of α.

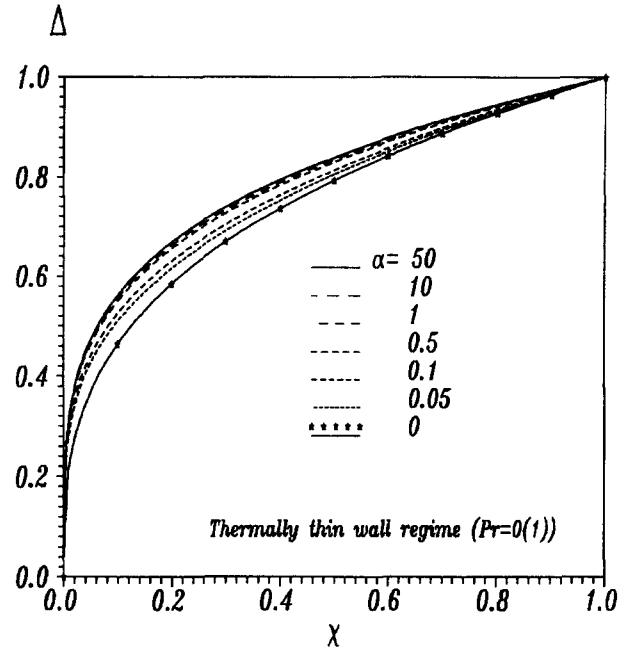

Figure 3 Nondimensional condensed layer thickness as a function of χ for different values of α

In the limit of Pr of order unity and $Ja \to 0$, the average Nusselt number

$$\overline{Nu} = \int_0^1 Nu(\chi)d\chi = 1 \tag{70}$$

is always unity for the same reasons mentioned above. For nonzero values of α, the local Nusselt number shows a singularity as $\chi \to 0$. As the value of α decreases, the local Nusselt number decreases faster in χ to values close to unity, showing the appearance of a boundary layer close to the leading edge.

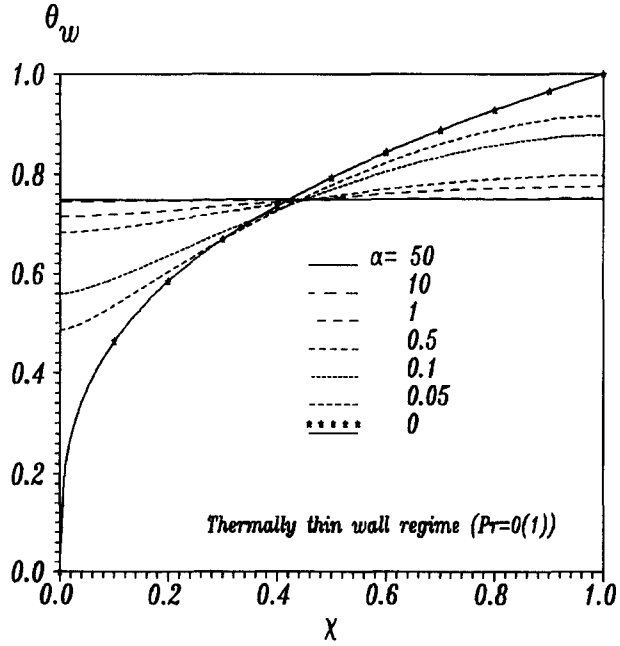

Figure 2 Nondimensional plate temperature profiles as a function of χ for different values of α

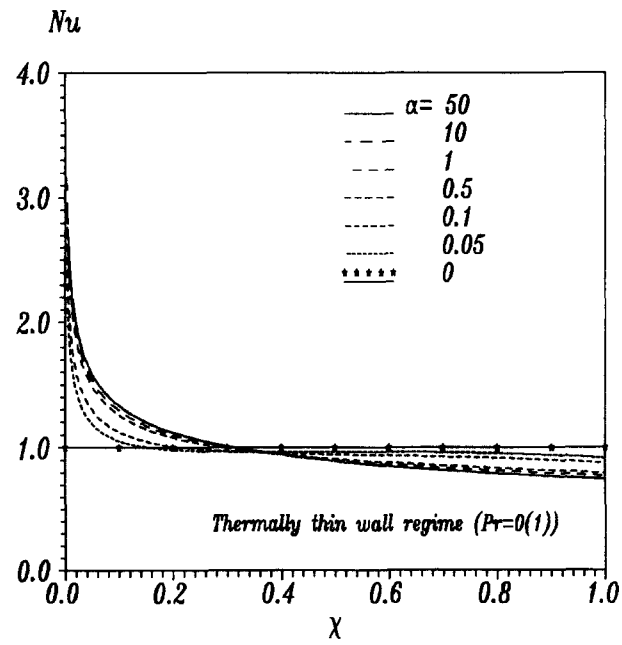

Figure 4 Nusselt number as a function of χ for different values of α

By way of illustration, we did some calculations using copper and stainless steel for the condensation process of saturated water at atmospheric pressures. We used the following parameters: $q_e = 100 KW/m^2$, $L = 1m$ and a Prandtl number for the condensed film of Pr = 2.3538. The resulting Jakob number is for this case, Ja = 0.06193. Table 1 gives the resulting values of Ja, α, α/ε^2, for different values of h. As we can see, the values of α in all cases are very small compared with unity. However, for copper material, the values of α/ε^2 are very large compared with unity (thermally thin wall), and the appropriate formulas to be used are given by Equations 67 to 69. Otherwise, for stainless steel, the appropriate regime is the thermally thick wall, where the equivalent formulas are given by Equation A8 in the Appendix B. In both cases, the temperature in physical units at $z = -1$ are given by

$$T_w = T_s - \chi^{1/3}\left(1 + \frac{\mathrm{JaPr}}{540}\chi^{4/3}\right)\frac{Lq_e}{\lambda_l}\left(\frac{\mathrm{Ja}}{\gamma}\right)^{1/4}$$

$$\approx T_s - 20.77\chi^{1/3}(1 + 0.00021\chi^{4/3}) \qquad (71)$$

for the thermally thin wall regime with $\alpha \to 0$ and

$$T_w = T_s - \left(\chi^{1/3} + \frac{\varepsilon^2}{\sigma}\right)\frac{Lq_e}{\lambda_l}\left(\frac{\mathrm{Ja}}{\gamma}\right)^{1/4} \approx T_s - 20.77\left(\chi^{1/3} + \frac{\varepsilon^2}{\alpha}\right) \qquad (72)$$

for the thermally thick wall regime. In the former case, the temperature distribution at $z = -1$ doesn't depend on the thickness of the plate. Otherwise, for the latter case, the ε^2/α is a linear function of the plate thickness and therefore, the influence is stronger.

In this paper, the condensation process of a saturated vapor in contact with one surface of a thin vertical plate has been analyzed for small values of the Jakob number, using asymptotic as well as numerical techniques. A uniform prescribed heat flux is assumed at the other vertical surface of the plate. The finite thermal conductivity of the plate material allows for transference of heat by conduction upstream through the plate, thus changing the mathematical character of the problem from parabolic to elliptic. Assuming the plate to have adiabatic leading (upper) and trailing (lower) edges, the heat convection through the lateral surface of the plate, affected by the axial heat conduction, governs the space evolution of the plate temperature, the condensed layer thickness, and the overall condensed fluid mass flow rate. The two asymptotic limits of large and small values of the parameter α, defined by the ratio of the fluid thermal resistance to that of the plate, have been analyzed for this condensation process. For large values of the parameter α, the plate temperature varies little in the longitudinal direction, thus producing a singular behavior for the local Nusselt number close to the leading edge. The leading solution in this limit reproduces the classical results of Nusselt for constant plate temperature. As the value of α decreases, the plate temperature comes closer to the temperature of the saturated vapor, reaching exactly this value for $\alpha = 0$. Because we prescribe the external heat flux, the longitudinal heat conduction through the plate has a minor influence on the thickness of the condensed film. The influence is bigger for the temperature distribution and the local Nusselt number. For very small Jakob numbers and Prandtl numbers of order unity, the solution is insensitive to the Prandtl number. However, as the Prandtl number increases, the main effect is to reduce the condensed film mass flow rate and thus the thickness of this layer. In this case, the convective terms in the energy equation have to be considered, changing the average Nusselt number, even in this case with known overall heat flux. We used asymptotic techniques to obtain a closed form solution for the plate temperature, thickness of the condensed film, and the local Nusselt numbers.

Table 1 Values of Ja, α, α/ε^2

Copper pure	α	α/ε^2	Stainless steel	α	α/ε^2
h=.01 m	.00105	10.5	h=.01 m	2.95×10^{-5}	.3952
.005	.00052	21	.005	1.97×10^{-5}	.7904
.0025	.00026	41.98	.0025	9.88×10^{-6}	1.581

Acknowledgments

This work has been supported by CONACyT.

Appendix A: Numerical solution of the evolution equation

In this appendix, we show the procedure used to solve numerically the evolution Equations 31. We transform the boundary value problem to a initial value problem by introducing the following variables

$$\phi = \left(\frac{4}{3}\right)^{\frac{8}{5}}\alpha^{\frac{4}{5}}Y; \chi = \left(\frac{4}{3}\right)^{\frac{1}{5}}\alpha^{\frac{3}{5}}s \qquad (A1)$$

The evolution equation now takes the parameter-free form

$$\frac{d^3Y}{ds^3} - \frac{1}{Y^{\frac{1}{4}}}\frac{dY}{ds} = -1 \qquad (A2)$$

with the initial conditions

$$Y(0) = \left.\frac{d^2Y}{ds^2}\right|_{s=0} = 0; \left.\frac{dY}{ds}\right|_{s=0} = C \qquad (A3)$$

where C is any value within a specified range. The corresponding values for the trailing edge of the plate can be obtained as we get

$$\left.\frac{d^2Y}{ds^2}\right|_{s=s_f} = 0 \qquad (A4)$$

Equation A2 is solved numerically suing a fourth-order Runge–Kutta technique with an integration step $\Delta s \sim s_f/1000$. Once we obtain s_f, we can compute α, and therefore the original variables ϕ and χ as

$$\alpha = \left(\frac{3}{4s_f^5}\right)^{\frac{1}{3}}; \chi = \frac{s}{s_f}; \phi = \left(\frac{4}{3s_f}\right)^{\frac{4}{3}}Y \qquad (A5)$$

Figure A1 shows the relationship of the initial slope $(dY/ds)_0 = C$, with the value of α. Thus, C must have values in the range $0 < C < 0.7944\ldots$ in order to achieve the adiabatic condition at

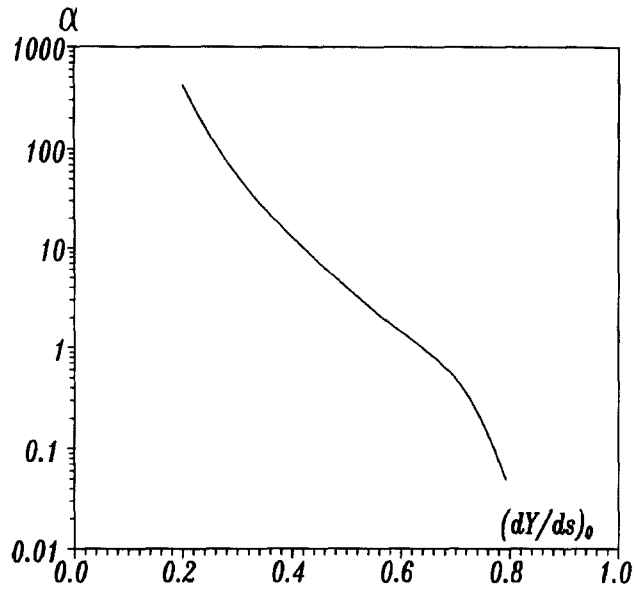

Figure A1 Initial slope $(dY/ds)_0$ as a function α

the trailing edge. The nondimensional plate temrperature is in this case

$$\theta_w = \frac{3d\phi}{4d\chi} = \left(\frac{4}{3s_f}\right)^{\frac{1}{3}} \frac{dY}{ds} \tag{A6}$$

Figure A2 shows the profiles for the d^2Y/ds^2, which is related to the temperature gradient at the plate as a function of s for different values of the initial slope. For values of C slightly larger than the critical value of $C = 0.7944\ldots$, we do not obtain the adiabatic condition at the trailing edge $d^2Y/ds^2 = 0$.

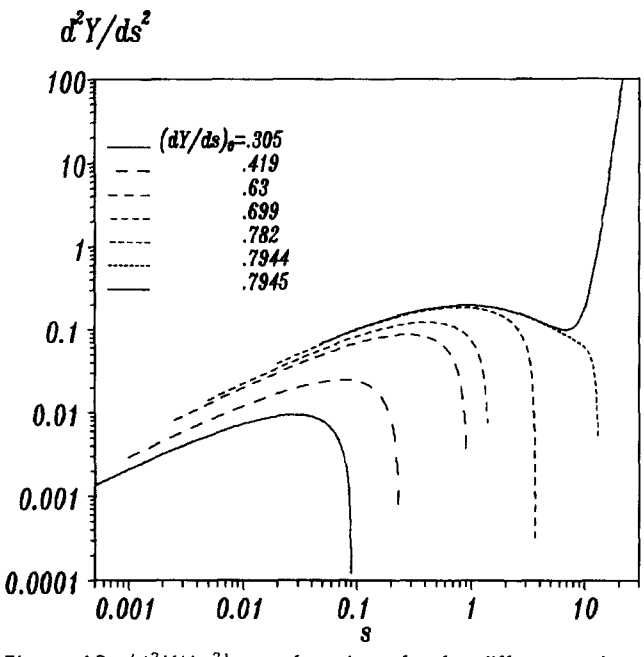

Figure A2 (d^2Y/ds^2) as a function of s for different values of the initial slopes $(dY/ds)_0$

Appendix B: Thermally thick wall approximation

For values of α/ε^2 of order unity, the nondimensional temperature variations n the plate in the transversal direction are very strong and are of the same order of magnitude as the overall temperature difference T_r. Therefore in this thermally thick wall regime, it is not justified to assume the plate temperature to be only a function of the longitudinal coordinate χ, but it is also a function of the transversal coordinate z. However, for small values of ε^2, the longitudinal heat conduction through the plate can be neglected, except in small regions close to both edges. Thus, the energy equation of the plate indicates a linear profile of the temperature in the z direction and a constant nondimensional temperature gradient

$$\frac{\partial\theta_w}{\partial z} = -\frac{\varepsilon^2}{\alpha} = \frac{\varepsilon^2}{\alpha\Delta}\frac{\partial\theta}{\partial\sigma}\bigg|_{\sigma=0} \tag{A7}$$

where we used the boundary conditions given by Equations 12 and 13. For Prandtl numbers of order unity and Ja $\to 0$ Equation 28 introduced in Equation A7 gives $\Delta(\chi) = \theta_w(\chi, z = 0)$. Thus, using Equation 18, we obtain

$$\Delta(\chi) = \chi^{\frac{1}{3}} \text{ and } \theta_w = \chi^{\frac{1}{3}} - \frac{\varepsilon^2}{\alpha} z \tag{A8}$$

References

Bromely L. A. 1952. Effect of heat capacity of condensate. *Ind. Eng. Chem.*, **44**, 2966–2969

Brouwers, H. J. H. 1989. Film condensation on nonisothermal vertical plates. *Int. J. Heat Mass Transfer*, **32**, 655–663.

Chen, M. M. 1961. An analytical study of laminar film condensation, Part 1, Flat plates. *J. Heat Transfer*, **83**, 48–54

Koh, J. C. Y., Sparrow E. M. and Hartnett J. P. 1961. The two-phase boundary layer in laminar film condensation. *Int. J. Heat Mass Transfer*, **2**, 69–82

Incropera. F. P. and DeWitt, D. P. 1990. *Fundamentals of Heat and Mass Transfer*, 3rd ed. Wiley, New York

Merte, H. 1973. Condensation heat transfer. *Adv. Heat Transfer*, **15**, 181–272

Nusselt, W. 1916. Die Oberflächenkondensation des Wasserdampfes, *Z. Ver. Dt. Ing.*, **60**, 541–546, 569–575

Patankar, S. V. and Sparrow, E. M. 1979. Condensation on an extended surface. *J. Heat Transfer*, **101**, 434–440

Rohsenow, W. M. 1956. Heat transfer and temperature distribution in laminar-film condensation. *Trans. ASME*, **78**, 1645–1648

Rose, J. W. 1988. Fundamentals of condensation heat transfer: Laminar film condensation. *JSME Int. J.*, **31**, 357–375

Sparrow, E. M. and Gregg, J. L. 1959. A boundary-layer treatment of laminar-film condensation. *Trans. ASME*, **81**, 13–17

Tanasawa, I. 1992. Advances in condensation heat transfer. *Adv. Heat Transfer*, **21**, 55–139

Wilkins, J. E. 1980. Condensation on an extended surface. *J. Heat Transfer*, **102**, 186–187